Performance of SC-FDE System in UWB Communications with Imperfect Channel Estimation

Yue Wang and Xiaodai Dong

Abstract: **Single carrier block transmission with frequency domain equalization (SC-FDE) has been shown to be a promising candidate in ultra-wideband (UWB) communications. In this paper, we analyze the performance of SC-FDE over UWB communications with channel estimation error. The probability density functions of the frequency domain minimum mean-squared error (MMSE) equalizer taps are derived in closed form. The error probabilities of single carrier block transmission with frequency domain MMSE equalization under imperfect channel estimation are presented and evaluated numerically. Compared with the simulation results, our semi-analytical analysis yields fairly accurate bit error rate performance, thus validating the use of the Gaussian approximation method in the performance analysis of the SC-FDE system with channel estimation error.**

Index Terms: **Channel estimation, single carrier block transmission with frequency domain equalization (SC-FDE), ultra-wideband (UWB).**

I. INTRODUCTION

Ultra-wideband (UWB) technology has received enormous attention in recent years for its potential to provide very high data rate communication with low power consumption. Recently, single carrier block transmission with frequency domain minimum mean-squared error (MMSE) equalization (SC-FDE) has been shown in [1] to have an overall performance advantage over the currently proposed multicarrier UWB (MC-UWB) employing OFDM [2] and impulse based single carrier UWB [3], especially when implementation issues such as power consumption and system complexity are taken into consideration. The performance of SC-FDE system was presented in [1], based on the assumption of perfect channel state information (CSI). However, this is not the case in reality since channel state information is only available through estimation algorithms with inherent channel estimation error. Despite the practical interest and importance of evaluating the effect of channel estimation error, the bit error rate (BER) of the SC-FDE system in UWB channels in the presence of channel estimation error has not been investigated. In this paper, we study the BER performance of single carrier block transmission with frequency domain MMSE equalization over UWB channels, with imperfect channel state information obtained from frequency domain least-square (LS) channel estimation algorithm.

Performance analysis of communication systems with channel estimation error is a subject of plenty research interests [4]–[7]. These analyses, however, were based on the intersymbol interference (ISI) free transmission, which cannot be applied to the SC-FDE system with frequency domain MMSE equalization. When MMSE equalization is performed in the frequency domain while signal detection is carried out in the time domain, all the other transmitted bits within one block will affect the detection of the current bit, resulting in complicated sums of decision variables and therefore it is not ISI free [1]. Assuming perfect CSI, ISI was approximated as Gaussian random variable (r.v.), which led to a simple and accurate analysis in [1]. In this paper, we study the more complicated performance problem for SC-FDE systems with imperfect channel estimation in UWB channels. Our analysis starts with the derivation of the pdf of frequency domain MMSE equalizer with channel estimation error. The BER performance of SC-FDE over UWB communications with imperfect channel estimation is then derived by employing the central limit theorem (CLT).

The remainder of this paper is organized as follows. Section II presents a brief description of the SC-FDE system model. Section III derives the pdf of the frequency domain equalizer taps. In Section IV, the newly derived pdf is applied to the BER analysis of the SC-FDE system over UWB communications with channel estimation error. Numerical results and discussions are presented in Section V. Section VI concludes this paper.

II. SC-FDE SYSTEM MODEL

We consider the cyclic prefixed single carrier block transmission with frequency domain equalization over ultra-wideband channels, where blocks of signals x_m $(0 \leq m \leq N-1)$ with length N are transmitted. Cyclic prefix (CP) of sufficient length is inserted between blocks to eliminate the inter-block interference (IBI).

Suppose that the T-spaced equivalent channel impulse response is of order L with taps $\mathbf{h} = [h(0), \cdots, h(L-1)]^T$. The frequency domain received signal $\mathbf{Y}$ can be expressed as [1]

$$\mathbf{Y} = \Lambda \mathbf{F}\mathbf{x} + \mathbf{F}\mathbf{n} \tag{1}$$

where $\mathbf{x} = [x_0, x_1, \cdots, x_{N-1}]^T$. Each element in the $N \times 1$ noise vector $\mathbf{n}$ is a Gaussian r.v. with variance $\sigma_n^2 = \frac{N_0}{2}$, where N_0 is the one-sided noise power spectral density. Moreover, $\mathbf{F}$ is the discrete Fourier transform (DFT) matrix and $F_{l,k} = \frac{1}{\sqrt{N}}\exp\{-j\frac{2\pi}{N}lk\}$, $0 \leq l,\ k \leq N-1$. Matrix Λ is a diagonal matrix with its kth entry as H_k, where H_k is the kth channel attenuation factor and $H_k = \sum_{l=0}^{L-1} h(l)\exp\{-j\frac{2\pi lk}{N}\}$.

The receiver performs frequency domain channel estimation. The estimated channel attenuation factors are utilized for the subsequent frequency domain equalizer to eliminate ISI within

Manuscript received September 27, 2005; approved for publication by Yong Soo Cho, Division II Editor, November 1, 2007.

Y. Wang is with the Advanced Wireless Research Group at Toshiba Research Europe Ltd., Bristol, UK, BS1 4ND, email: yue.wang@toshiba-trel.com.

X. Dong is with the Department of Electrical and Computer Engineering, University of Victoria, BC, Canada, V8W 3P6, email: xdong@ece.uvic.ca.

1229-2370/07/$10.00 © 2007 KICS

the individual transmission blocks. Denote the estimated channel attenuation factors as $\hat{\mathbf{H}} = [\hat{H}_0, \hat{H}_1, \cdots, \hat{H}_{N-1}]^T$, the commonly used frequency domain MMSE equalization taps can be expressed as [8]

$$C_k = \frac{\hat{H}_k^*}{|\hat{H}_k|^2 + B} \tag{2}$$

where $B = \sigma_n^2/\sigma_b^2$ is the inverse of the signal-to-noise ratio (SNR), and σ_b^2 is the average energy per bit of the transmitted data. It is assumed that the value of SNR is available at the receiver.

After frequency domain equalization and inverse discrete Fourier transform, the received signal $\mathbf{z}$ becomes [1]

$$\mathbf{z} = \mathbf{F}^H \mathbf{C} \Lambda \mathbf{F} \mathbf{x} + \mathbf{F}^H \mathbf{C} \mathbf{F} \mathbf{n} \tag{3}$$

where $\mathbf{C}$ is an $N \times N$ diagonal matrix with its kth diagonal element as the frequency domain equalizer tap C_k, $k = 0, \cdots, N-1$. Signal detection is performed in the time domain. We consider the detection of bit x_m, $m = 0, 1, \cdots, N-1$, which can be obtained from z_m as [1]

$$z_m = \frac{1}{N} \sum_{k=0}^{N-1} C_k H_k x_m + \frac{1}{N} \sum_{\substack{l=0 \\ l \neq m}}^{N-1} \left(\sum_{k=0}^{N-1} H_k C_k e^{-\frac{j2\pi(l-m)k}{N}} \right) x_l + \frac{1}{N} \sum_{l=0}^{N-1} \left(\sum_{k=0}^{N-1} C_k e^{-\frac{j2\pi(l-m)k}{N}} \right) n_l. \tag{4}$$

When BPSK modulation is considered, the detected block becomes

$$\hat{\mathbf{x}} = \text{sgn}(\mathbf{z}) \tag{5}$$

where $\text{sgn}(\cdot)$ is the algebraic sign function. Fig. 1 shows the block diagram of the investigated SC-FDE system.

III. PROBABILITY DENSITY FUNCTIONS OF THE FREQUENCY DOMAIN EQUALIZER TAPS

In this section, we present the pdf of the frequency domain MMSE channel equalizer taps with imperfect CSI, where the estimated channel attenuation factors $\hat{H}_k$ $(k = 0, \cdots, N-1)$ are obtained by frequency domain LS channel estimation algorithms. Suppose one block of pilot symbols $\mathbf{p}$ is transmitted for channel estimation purpose. Following (1), the frequency domain received signal can be rewritten as [1]

$$\mathbf{Y} = \mathbf{P}\mathbf{H} + \mathbf{N}_p \tag{6}$$

where $\mathbf{P}$ is a diagonal matrix with its kth diagonal element P_k as the kth DFT coefficient of the pilot sequences $\mathbf{p}$, and $\mathbf{N}_p = \mathbf{F}\mathbf{n}_p$ is an $N \times 1$ column vector with its kth element N_{p_k} being the kth DFT coefficient of the sampled noise vector of the pilot block.

The channel attenuation factors estimated by the LS algorithm can be obtained as

$$\hat{H}_k = \frac{Y_k}{P_k} = H_k + \frac{N_{p_k}}{P_k} \tag{7}$$

for $k = 0, 1, \cdots, N-1$, and

$$N_{p_k} = \frac{1}{\sqrt{N}} \sum_{l=0}^{N-1} n_{p_l} \exp\left(-\frac{j2\pi lk}{N} \right). \tag{8}$$

Hence, N_{p_k} is a complex Gaussian r.v. with zero mean and variance $\sigma_n^2 = \frac{N_0}{2}$. Furthermore, the real and imaginary part of N_{p_k} are uncorrelated Gaussian r.v. with zero mean and variance $\frac{\sigma_n^2}{2} = \frac{N_0}{4}$. Denote the real and imaginary part of $\hat{H}_k$ as R_k and I_k, respectively. We have from (7) that R_k and I_k are uncorrelated Gaussian r.v. and $R_k \sim \mathbb{N}(H_{kr}, \frac{N_0}{4|P_k|^2})$, $I_k \sim \mathbb{N}(H_{ki}, \frac{N_0}{4|P_k|^2})$, where $\mathbb{N}(\mu, \sigma^2)$ denotes the normal distribution with mean μ and variance σ^2, and H_{kr} and H_{ki} denote the real and imaginary part of H_k, respectively.

Note that since $\hat{H}_k$'s $(k = 0, \cdots, N-1)$ are independent r.v.'s, C_k's $(k = 0, \cdots, N-1)$ are also independent. In the derivation that follows, we use the notation of $\mu_k = \mathbb{E}[\hat{H}_k] = \mu_{kr} + j\mu_{ki}$ and $\sigma_k^2 = \mathbb{E}\left[\left| \hat{H}_k - \mu_k \right|^2 \right]$. Therefore, for LS channel estimation, we have $\mu_{kr} = H_{kr}$, $\mu_{ki} = H_{ki}$, and $\sigma_k^2 = \frac{N_0}{4|P_k|^2}$.

Since the real and imaginary part of $\hat{H}_k$ are uncorrelated Gaussian, the joint pdf of R_k and I_k is given by [10]

$$f_{R_k, I_k}(R_k, I_k) = \frac{1}{2\pi\sigma_k^2} e^{-\frac{(R_k - \mu_{kr})^2 + (I_k - \mu_{ki})^2}{2\sigma_k^2}}. \tag{9}$$

Following (2), the MMSE frequency domain equalizer taps can be rewritten as

$$C_k = \frac{R_k - jI_k}{R_k^2 + I_k^2 + B} = r_k e^{j\theta_k} \tag{10}$$

where

$$r_k = \frac{\sqrt{R_k^2 + I_k^2}}{R_k^2 + I_k^2 + B} \tag{11}$$

$$\theta_k = -\tan^{-1} \frac{I_k}{R_k}. \tag{12}$$

Or equivalently,

$$r_k \cos\theta_k = \frac{R_k}{R_k^2 + I_k^2 + B} \tag{13}$$

and

$$r_k \sin\theta_k = -\frac{I_k}{R_k^2 + I_k^2 + B}. \tag{14}$$

The joint pdf of (r_k, θ_k) can be obtained as [10]

$$f_{r_k, \theta_k}(r_k, \theta_k) = \sum_i \frac{1}{|\mathbf{J}_i|} f_{R_k, I_k}(R_{k_i}, I_{k_i}) \tag{15}$$

where R_{k_i} and I_{k_i} are the ith solution of (11) and (12), and $|\cdot|$ denotes absolute value of the determinant $\mathbf{J}_i$

$$\mathbf{J}_i = \begin{vmatrix} \frac{\partial r_k}{\partial R_k} & \frac{\partial r_k}{\partial I_k} \\ \frac{\partial \theta_k}{\partial R_k} & \frac{\partial \theta_k}{\partial I_k} \end{vmatrix}_{R_k = R_{k_i}, I_k = I_{k_i}} = \left. \frac{B - R_k^2 - I_k^2}{(R_k^2 + I_k^2)^{1/2} (R_k^2 + I_k^2 + B)^2} \right|_{R_k = R_{k_i}, I_k = I_{k_i}}. \tag{16}$$

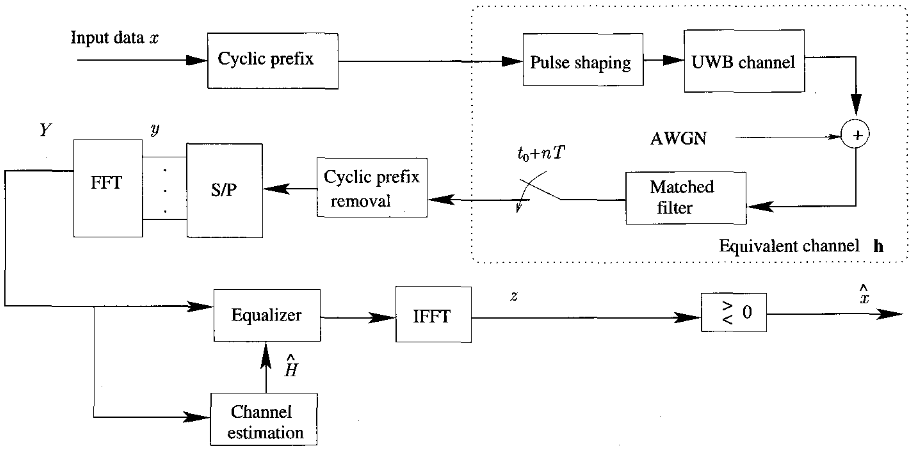

Fig. 1. SC-FDE system.

By mathematical derivations, we solve $R_{k_i}^2 + I_{k_i}^2$ from (11) and (12) as

$$R_{k_i}^2 + I_{k_i}^2 = \frac{1 - 2Br_k^2 \pm \sqrt{1 - 4Br_k^2}}{2r_k^2} \tag{17}$$

where $\pm$ applies to $i = 1$ and $i = 2$, respectively. Converting to the polar coordinate form, (17) results in

$$\frac{1}{|\mathbf{J}_i|} = \frac{1}{2r_k^3\sqrt{1 - 4Br_k^2}}\left(1 - 2Br_k^2 \pm \sqrt{1 - 4Br_k^2}\right). \tag{18}$$

Therefore, the pdf of the kth frequency domain channel equalizer tap can be obtained as (19) on top of next page, where $f_{R_k,I_k}(\cdot)$ is the joint pdf of the kth estimated channel attenuation factor $\hat{H}_k$ given by (9), which can be rewritten in the polar coordinate form as

$$f_{R_k,I_k}(r_{k_i}, \theta_{k_i}) = \frac{1}{2\pi\sigma_k^2} e^{-\frac{|\mu_k|^2 - B}{2\sigma_k^2}} \times e^{-\frac{\left(1 \pm \sqrt{1 - 4Br_k^2}\right)\left(1 - 2|\mu_k| r_k \cos(\theta_k + \varphi_k)\right)}{4\sigma_k^2 r_k^2}} \tag{20}$$

where $|\mu_k|$ and φ_k are the norm and phase of μ_k, respectively.

Applying (20) to (19), the joint density of (r_k, θ_k) can be obtained in closed-form as (21) on top of next page.

IV. PERFORMANCE ANALYSIS

In this section, we apply the pdf of the MMSE frequency domain channel equalizer taps to the derivation of the BER performance. Conditional on the channel impulse response $\mathbf{h}$, the probability of error for the detection of the mth bit is given by

$$\mathrm{P}_m(e|\mathbf{h}) = \Pr(z_m > 0 | x_m = -1, \mathbf{h}). \tag{22}$$

Given $x_m = -1$, we obtain (23) from (4) as shown on top of next page, where X_k is the Fourier coefficients of one transmitted block x_i, $i = 0, 1, \cdots, N-1$, independent of C_k and N_k. The second to last equality in (23) is obtained by applying

$$X_k = \frac{1}{\sqrt{N}} \sum_{\substack{n=0 \\ n \neq m}}^{N-1} x_n e^{-\frac{j2\pi nk}{N}} - \frac{1}{\sqrt{N}} e^{-\frac{j2\pi mk}{N}}. \tag{24}$$

A. Mean and Variance of L

Denote $L_k = C_k(H_k X_k + N_k) e^{\frac{j2\pi mk}{N}}$. Note that since $\hat{H}_k$, $k = 0, \cdots, N-1$ are independent r.v.'s, $\{C_k\}$ are also independent of one another. The r.v.'s $\{X_k\}$ and $\{N_k\}$ are also independent for different k's. As the sum of N independent r.v.'s $\{L_k\}$, L can be modeled as a Gaussian r.v. with mean μ_L and variance σ_L^2. Since the noise sample N_{p_k} in C_k comes from the pilot block which is independent of N_k, C_k is independent of N_k. Therefore, it is straightforward to show that

$$\begin{aligned}\mu_L &= \frac{1}{\sqrt{N}} \sum_{k=0}^{N-1} \mathbb{E}\left[C_k(H_k X_k + N_k)\right] e^{\frac{j2\pi mk}{N}} \\ &= \frac{1}{\sqrt{N}} \sum_{k=0}^{N-1} \mathbb{E}\left[C_k\right] \{H_k \mathbb{E}\left[X_k\right] + \mathbb{E}\left[N_k\right]\} e^{\frac{j2\pi mk}{N}} \\ &= -\frac{1}{N} \sum_{k=0}^{N-1} H_k \mathbb{E}\left[C_k\right]\end{aligned} \tag{25}$$

where

$$\mathbb{E}\left[X_k\right] = -\frac{1}{\sqrt{N}} e^{-\frac{j2\pi mk}{N}} \tag{26}$$

is utilized in the last equality.

The variance of L can be obtained as

$$\sigma_L^2 = \mathbb{E}\left[|L|^2\right] - |\mu_L|^2 \tag{27}$$

where

$$\begin{aligned}\mathbb{E}\left[|L|^2\right] =& \frac{1}{N} \sum_{p=0}^{N-1} \sum_{q=0}^{N-1} \mathbb{E}\left[\left[C_p(H_p X_p + N_p)\right]\left[C_q^*(H_q^* X_q^* + N_q^*)\right]\right] e^{\frac{j2\pi m(p-q)}{N}} \\ =& \frac{1}{N} \sum_{p=0}^{N-1} \sum_{q=0}^{N-1} \mathbb{E}\left[C_p C_q^*\right] \mathbb{E}\left[(H_p X_p + N_p)(H_q^* X_q^* + N_q^*)\right] e^{\frac{j2\pi m(p-q)}{N}} \\ =& \frac{1}{N} \sum_{p=0}^{N-1} \sum_{q=0}^{N-1} \mathbb{E}\left[C_p C_q^*\right] \left[H_p H_q^* \mathbb{E}\left[X_p X_q^*\right] + \mathbb{E}\left[N_p N_q^*\right]\right] e^{\frac{j2\pi m(p-q)}{N}}.\end{aligned}$$

$$f_{r_k,\theta_k}(r_k,\theta_k) = \frac{1}{2r_k^3\sqrt{1-4Br_k^2}}\left[1-2Br_k^2+\sqrt{1-4Br_k^2}\right] f_{R_k,I_k}(R_{k_1},I_{k_1}) + \frac{1}{2r_k^3\sqrt{1-4Br_k^2}}\left[1-2Br_k^2-\sqrt{1-4Br_k^2}\right] f_{R_k,I_k}(R_{k_2},I_{k_2}). \tag{19}$$

$$f_{r_k,\theta_k}(r_k,\theta_k) = \frac{1}{4\pi\sigma_k^2}\mathrm{e}^{-\frac{|\mu_k|^2-B}{2\sigma_k^2}} \times \frac{1}{r_k^3\sqrt{1-4Br_k^2}}\left[\left(1-2Br_k^2+\sqrt{1-4Br_k^2}\right)\mathrm{e}^{-\frac{\left(1+\sqrt{1-4Br_k^2}\right)\left(1-2|\mu_k|r_k\cos(\theta_k+\varphi_k)\right)}{4\sigma_k^2 r_k^2}} + \left(1-2Br_k^2-\sqrt{1-4Br_k^2}\right)\mathrm{e}^{-\frac{\left(1-\sqrt{1-4Br_k^2}\right)\left(1-2|\mu_k|r_k\cos(\theta_k+\varphi_k)\right)}{4\sigma_k^2 r_k^2}}\right]. \tag{21}$$

$$\begin{aligned} L = z_m|x_m = -1 &= -\frac{1}{N}\sum_{k=0}^{N-1} C_k H_k + \frac{1}{N}\sum_{\substack{l=0\\ l\neq m}}^{N-1}\left(\sum_{k=0}^{N-1} H_k C_k \mathrm{e}^{-\frac{j2\pi(l-m)k}{N}}\right)x_l + \frac{1}{N}\sum_{l=0}^{N-1}\left(\sum_{k=0}^{N-1} C_k \mathrm{e}^{-\frac{j2\pi(l-m)k}{N}}\right)n_l \\ &= -\frac{1}{N}\sum_{k=0}^{N-1} C_k H_k + \frac{1}{N}\sum_{k=0}^{N-1} C_k H_k \mathrm{e}^{\frac{j2\pi mk}{N}}\sum_{\substack{l=0\\ l\neq m}}^{N-1}\mathrm{e}^{-\frac{j2\pi lk}{N}}x_l + \frac{1}{\sqrt{N}}\sum_{k=0}^{N-1} C_k N_k \mathrm{e}^{\frac{j2\pi mk}{N}} \\ &= \frac{1}{\sqrt{N}}\sum_{k=0}^{N-1} C_k H_k X_k \mathrm{e}^{\frac{j2\pi mk}{N}} + \frac{1}{\sqrt{N}}\sum_{k=0}^{N-1} C_k N_k \mathrm{e}^{\frac{j2\pi mk}{N}} = \frac{1}{\sqrt{N}}\sum_{k=0}^{N-1} C_k (H_k X_k + N_k)\mathrm{e}^{\frac{j2\pi mk}{N}}. \end{aligned} \tag{23}$$

Since

$$\mathbb{E}\left[X_p X_q^*\right] = \begin{cases} 1, & p = q, \\ 0, & p \neq q, \end{cases}$$

and

$$\mathbb{E}\left[N_p N_q^*\right] = \begin{cases} \sigma_n^2, & p = q, \\ 0, & p \neq q, \end{cases}$$

we have (28) as shown on top of next page, and

$$\mathbb{E}\left[|L|^2\right] = \frac{1}{N}\sum_{p=0}^{N-1}\mathbb{E}\left[|C_p|^2\right]\left[|H_p|^2+\sigma_n^2\right]. \tag{29}$$

Applying (25) and (29) to (27), the variance of L can be obtained.

B. Error Probabilities

Having obtained the mean and variance of L, the conditional error probability on $\mathbf{h}$ for the detection of the mth bit within a block can be calculated from (22) as

$$\mathrm{P}_m(e|\mathbf{h}) = \mathbf{Q}\left(-\frac{\mu_L}{\sigma_L}\right). \tag{30}$$

To calculate (30), we need to calculate the values of $\mathbb{E}[C_k]$ and $\mathbb{E}\left[|C_k|^2\right]$. Applying the pdf of C_k obtained in Section III, we show in Appendix A the detailed derivation of $\mathbb{E}[C_k]$ as an example. The calculation of $\mathbb{E}\left[|C_k|^2\right]$ follows exactly the same manner as in Appendix A. In summary,

$$\mathbb{E}[C_k] = \frac{1}{\sqrt{2}\sigma_k}\mathrm{e}^{-j\phi_k}\mathrm{e}^{-\frac{|\mu_k|^2}{2\sigma_k^2}}\Psi_k\left(\frac{1}{2},1,1\right) \tag{31}$$

and

$$\mathbb{E}\left[|C_k|^2\right] = \frac{1}{2\sigma_k^2}\mathrm{e}^{-\frac{|\mu_k|^2}{2\sigma_k^2}}\Psi_k(1,2,0) \tag{32}$$

where

$$\Psi_k(\varsigma,\tau,\upsilon) = \int_0^\infty \frac{u^\varsigma}{\left(u+\frac{|P_k|^2}{\sigma_b^2}\right)^\tau}\mathrm{e}^{-u}\mathrm{I}_\upsilon(\eta_k\sqrt{u})du \tag{33}$$

with $\eta_k = \frac{\sqrt{2}|\mu_k|}{\sigma_k}$ and $\mathrm{I}_\upsilon(\cdot)$ is the υth order modified Bessel function of the first kind.

The conditional error probability (30) for the detection of a certain bit x_m within a block can therefore be evaluated with (25), (27), (29), (31), and (32). The bit error rate of one block conditional on channel gains is then calculated by averaging $\mathrm{P}_m(e|\mathbf{h})$ over the block, and the unconditional probability of error for SC-FDE is obtained by averaging the conditional error probability over 100 UWB channel realizations for a particular channel model.

$$\mathbb{E}\left[C_pC_q^*\right]\left[H_pH_q^*\mathbb{E}\left[X_pX_q^*\right]+\mathbb{E}(N_pN_q^*)\right]=\begin{cases}\mathbb{E}\left[|C_p|^2\right]\left[|H_p|^2+\sigma_n^2\right], & p=q,\\ 0, & p\neq q.\end{cases} \tag{28}$$

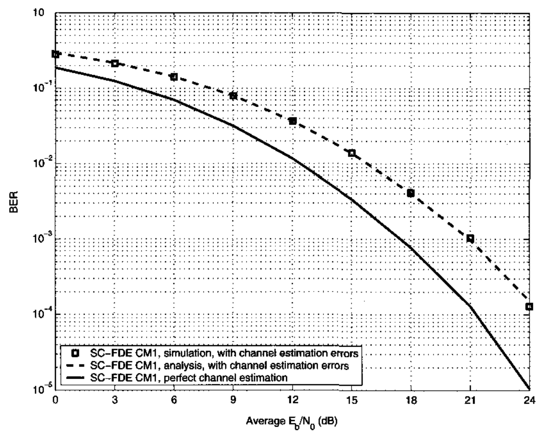

Fig. 2. Average BER performance of SC-FDE with channel estimation error over the UWB channel CM1.

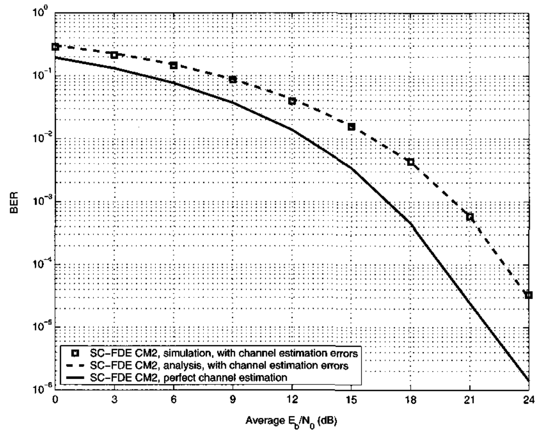

Fig. 3. Average BER performance of SC-FDE with channel estimation error over the UWB channel CM2.

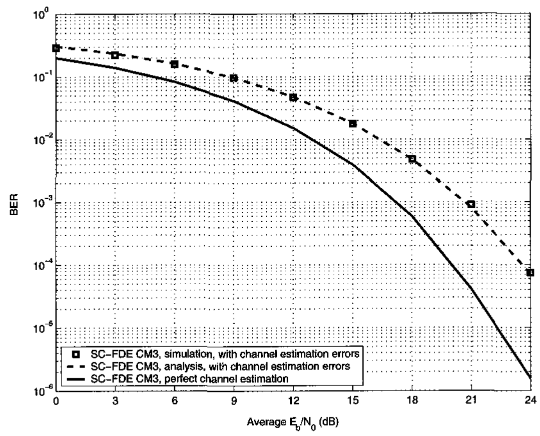

Fig. 4. Average BER performance of SC-FDE with channel estimation error over the UWB channel CM3.

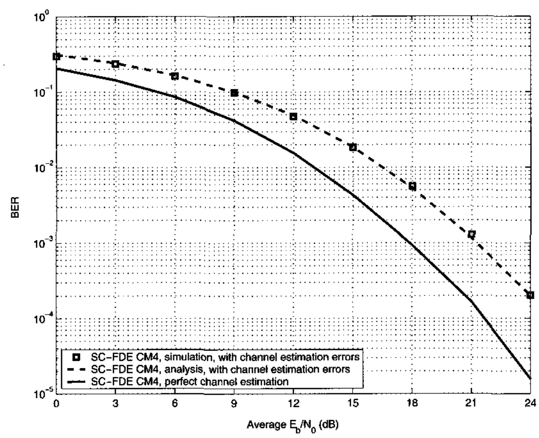

Fig. 5. Average BER performance of SC-FDE with channel estimation error over the UWB channel CM4.

V. NUMERICAL EXAMPLES AND DISCUSSIONS

A. Numerical examples

In this section, the error probabilities of SC-FDE system with frequency domain LS channel estimation error over various UWB channel models are evaluated numerically and compared with the simulation results. The investigated SC-FDE system follows that in [1] where a data block length $N=256$ is used, with CP length of 64 and the effective data rate of 400 Mbps. The root raised cosine (RRC) pulse with roll off factor $\beta=0.5$ is employed as the pulse shaping filter. The UWB channels used are CM1–CM4 channel models proposed by the IEEE 802.15.3a study group [11]. In both numerical evaluation and simulations, the transmitted pulse shaping filter, the receiver matched filter and one of the 100 channel realizations for a particular UWB channel model are convolved to form 100 different equivalent channel realizations over which the BER's are averaged.

The semi-analytical results of BER performance of SC-FDE over UWB channels with frequency domain LS channel estimations are shown in Figs. 2–5, where one block of optimal pilot sequence is utilized [1]. That is, the pilot sequence has a flat spectrum with its DFT coefficients being constant ones, $|P_k|=1$ for $k=0,1,\cdots,N-1$. Our results show that, compared to the simulation results, Gaussian approximation yields fairly close BER performance to that of the SC-FDE system with frequency domain MMSE equalization under imperfect channel estimation, thus validating its use. Furthermore, a performance degradation of around 3 dB can be observed compared to the performance of SC-FDE with perfect channel state information.

VI. CONCLUSION

The impact of channel estimation error on the performance of SC-FDE system over UWB channels has been investigated in this paper. A general analysis method for the BER performance of SC-FDE with channel estimation error has been presented. The BER expression for the SC-FDE system conditioned on the UWB channel has been derived and evaluated numerically. Our results have validated the utilization of the Gaussian approximation method in the performance evaluation for the single carrier block transmission with frequency domain MMSE equalizations and LS channel estimation error over UWB channels.

APPENDIX A

In this appendix, we derive the expression for $\xi_{1k} = \mathbb{E}[C_k]$. We know from (10) and (21) that

$$\Omega = \mathbb{E}[C_k] = \int_{r_k}\int_{\theta_k} r_k e^{j\theta_k} f_{r_k,\theta_k}(r_k,\theta_k) dr_k d\theta_k. \quad (34)$$

Denote

$$\rho_{\pm}(r_k) = \frac{1-2Br_k^2 \pm \sqrt{1-4Br_k^2}}{r_k^3\sqrt{1-4Br_k^2}} \quad (35)$$

and

$$\lambda_{\pm}(r_k) = \frac{1 \pm \sqrt{1-4Br_k^2}}{4r_k^2\sigma_k^2}. \quad (36)$$

Eq. (34) can be rewritten as

$$\begin{aligned}\Omega =& \frac{1}{4\pi\sigma_k^2} e^{-\frac{|\mu_k|^2-B}{2\sigma_k^2}} \times \\ &\left\{\int_{r_k}\int_{\theta_k} r_k\rho_{+}(r_k) e^{j\theta_k-\lambda_{+}(r_k)(1-2|\mu_k|r_k\cos(\theta_k+\phi_k))}\right. \\ &\left.+\int_{r_k}\int_{\theta_k} r_k\rho_{-}(r_k) e^{j\theta_k-\lambda_{-}(r_k)(1-2|\mu_k|r_k\cos(\theta_k+\phi_k))}\right\} dr_k d\theta_k \\ =& \frac{1}{4\pi\sigma_k^2} e^{-\frac{|\mu_k|^2-B}{2\sigma_k^2}} (\Omega_1+\Omega_2) \end{aligned} \quad (37)$$

where

$$\begin{aligned}\Omega_{1,2} =& \int_{r_k} r_k\rho_{\pm}(r_k) e^{-\lambda_{\pm}(r_k)} \\ &\times \int_0^{2\pi} e^{j\theta_k+2\lambda_{\pm}(r_k)|\mu_k|r_k\cos(\theta_k+\phi_k)} d\theta_k dr_k \end{aligned} \quad (38)$$

and the sign $\pm$ applies to Ω_1 and Ω_2, respectively. Note that the inner integral in Ω_1 and Ω_2 can be simplified to

$$\begin{aligned}\Omega_\theta =& \int_0^{2\pi} e^{j\theta_k+2\lambda_{\pm}(r_k)|\mu_k|r_k\cos(\theta_k+\phi_k)} d\theta_k \\ =& e^{-j\phi_k}\int_0^{2\pi} e^{j(\theta_k+\phi_k)+2\lambda_{\pm}(r_k)|\mu_k|r_k\cos(\theta_k+\phi_k)} d\theta_k \\ =& 2\pi e^{-j\phi_k} I_1\left(2\lambda_{\pm}(r_k)|\mu_k|r_k\right) \end{aligned} \quad (39)$$

where $I_n(\cdot)$ is the nth order modified Bessel function of the first kind.

The first integral Ω_1 in (37) now becomes

$$\begin{aligned}\Omega_1 =& 2\pi e^{-j\phi_k}\int_{r_k} r_k\rho_{+}(r_k) e^{-\lambda_{+}(r_k)} I_1\left(2\lambda_{+}(r_k)|\mu_k|r_k\right) dr_k \\ =& 2\pi e^{-j\phi_k}\int_{r_k} \frac{1-2Br_k^2+\sqrt{1-4Br_k^2}}{r_k^2\sqrt{1-4Br_k^2}} \\ &\times I_1\left(\frac{|\mu_k|\left(1+\sqrt{1-4Br_k^2}\right)}{2\sigma_k^2 r_k}\right) e^{-\frac{1+\sqrt{1-4Br_k^2}}{4r_k^2\sigma_k^2}} dr_k. \end{aligned} \quad (40)$$

By making a change of variable in (40) as

$$t = \frac{|\mu_k|\left(1+\sqrt{1-4Br_k^2}\right)}{2\sigma_k^2 r_k}, \quad (41)$$

we have

$$r_k = \frac{t\sigma_k^2|\mu_k|}{t^2\sigma_k^4+B|\mu_k|^2} \quad (42)$$

and

$$dr_k = \sigma_k^2|\mu_k|\frac{B|\mu_k|^2-t^2\sigma_k^4}{(t^2\sigma_k^4+B|\mu_k|^2)^2}. \quad (43)$$

Furthermore, since

$$r_k = \frac{\sqrt{R_k^2+I_k^2}}{R_k^2+I_k^2+B}, \quad (44)$$

there is $r_k \in (0, \frac{1}{2\sqrt{B}})$. Therefore, $t \in \left(\infty, \frac{\sqrt{B}|\mu_k|}{\sigma_k^2}\right)$ and

$$\Omega_1 = \frac{4\pi\sigma_k^2}{|\mu_k|} e^{-j\phi_k} e^{-\frac{B}{2\sigma_k^2}} \int_{\frac{\sqrt{B}|\mu_k|}{\sigma_k^2}}^{\infty} \frac{t^2}{t^2+\frac{B|\mu_k|^2}{\sigma_k^4}} I_1(t) e^{-\frac{\sigma_k^2}{2|\mu_k|^2}t^2} dt. \quad (45)$$

Similarly, we have

$$\begin{aligned}\Omega_2 =& 2\pi e^{-j\phi_k}\int_{r_k} \frac{1-2Br_k^2-\sqrt{1-4Br_k^2}}{r_k^2\sqrt{1-4Br_k^2}} \\ &\times I_1\left(\frac{|\mu_k|\left(1-\sqrt{1-4Br_k^2}\right)}{2\sigma_k^2 r_k}\right) e^{-\frac{1-\sqrt{1-4Br_k^2}}{4r^2\sigma_k^2}} dr_k. \end{aligned} \quad (46)$$

By a change of variable in (46)

$$t = \frac{|\mu_k|\left(1-\sqrt{1-4Br_k^2}\right)}{2\sigma_k^2 r_k} \quad (47)$$

where $t \in \left(0, \frac{\sqrt{B}|\mu_k|}{\sigma_k^2}\right)$, the second integral Ω_2 in (37) can be rewritten as

$$\Omega_2 = \frac{4\pi\sigma_k^2}{|\mu_k|} e^{-j\phi_k} e^{-\frac{B}{2\sigma_k^2}} \int_0^{\frac{\sqrt{B}|\mu_k|}{\sigma_k^2}} \frac{t^2}{t^2\frac{B|\mu_k|^2}{\sigma_k^4}} I_1(t) e^{-\frac{\sigma_k^2}{2|\mu_k|^2}t^2} dt. \quad (48)$$

Applying (45) and (48) to (37) yields

$$\begin{aligned}\Omega &= \frac{1}{|\mu_k|}\mathrm{e}^{-j\phi_k}\mathrm{e}^{-\frac{|\mu_k|^2}{2\sigma_k^2}}\int_0^\infty \frac{t^2}{t^2+\frac{B|\mu_k|^2}{\sigma_k^4}}\mathrm{e}^{-\frac{\sigma_k^2}{2|\mu_k|^2}t^2}\mathrm{I}_1(t)dt \\ &= \frac{1}{\sqrt{2}\sigma_k}\mathrm{e}^{-j\phi_k}\mathrm{e}^{-\frac{|\mu_k|^2}{2\sigma_k^2}}\int_0^\infty \frac{\sqrt{u}}{u+\frac{|P_k|^2}{\sigma_b^2}}\mathrm{e}^{-u}\mathrm{I}_1\left(\eta_k\sqrt{u}\right)du \qquad (49)\end{aligned}$$

where $\eta_k = \frac{\sqrt{2}|\mu_k|}{\sigma_k}$ and a change of variable $u = \frac{\sigma_k^2}{2|\mu_k|^2}t^2$ has been made. Therefore, the final expression for (34) can be obtained as

$$\Omega = \mathbb{E}[C_k] = \frac{1}{\sqrt{2}\sigma_k}\mathrm{e}^{-j\phi_k}\mathrm{e}^{-\frac{|\mu_k|^2}{2\sigma_k^2}}\Psi_k(\frac{1}{2},1,1) \qquad (50)$$

where $\Psi_k(\cdot)$ is defined as

$$\Psi_k(\varsigma,\tau,\upsilon) = \int_0^\infty \frac{u^\varsigma}{\left(u+\frac{|P_k|^2}{\sigma_b^2}\right)^\tau}\mathrm{e}^{-u}\mathrm{I}_\upsilon(\eta_k\sqrt{u})du. \qquad (51)$$

REFERENCES

[1] Y. Wang, X. Dong, P. H. Wittke, and S. Mo, "Cyclic prefixed single carrier transmission in ultra-wideband communications," *IEEE Trans. Wireless Commun.*, vol. 5, pp. 2017–2021, Aug. 2006.

[2] IEEE P802.15.3a Working Group, P802.15-03/268r2, Multi-band OFDM physical layer proposal for IEEE 802.15 Task Group 3a, Nov. 2003.

[3] IEEE P802.15.3a Working Group, P802.15-04/0137r0, DS-UWB physical layer submission to 802.15 Task Group 3a, Mar. 2004.

[4] S. K. Wilson and J. M. Cioffi, "Probability density functions for analyzing multi-amplitude constellations in Rayleigh and Ricean channels," *IEEE Trans. Commun.*, vol. 47, pp. 380.386, Mar. 1999.

[5] Y. Ma, R. Schober, and S. Pasupathy, "Effect of imperfect channel estimation on MRC diversity in fading channels," in *Proc. IEEE ICC*, Paris, France, June 2004, pp. 3163–3167.

[6] X. Dong and N. C. Beaulieu, "SER of two-dimensional signalings in Rayleigh fading with channel estimation errors," in *Proc. IEEE ICC*, Seattle, USA., May 2003, pp. 2763–2767.

[7] X. Dong and L. Xiao, "Symbol error probability of two-dimensional signaling in Ricean fading with imperfect channel estimation," *IEEE Trans. Veh. Technol.*, vol. 54, pp. 538–549, Mar. 2005.

[8] H. Sari, G. Karam, and I. Jeanclaude, "Transmission techniques for digital terrestrial TV broadcasting," *IEEE Commun. Mag.*, vol. 33, pp. 100–109, Feb. 1995.

[9] Y. Wang and X. Dong, "Frequency domain channel estimation for SC-FDE in UWB communications," *IEEE Trans. Commun.*, vol. 54, pp. 2155–2163, Dec. 2006.

[10] A. Papoulis, *Probability, Random Variables, and Stochastic Processes.* New York, NY: McGraw-Hill, 1991.

[11] J. Foerster, Channel Modeling Subcommittee Report (Final). IEEE P802.15.3a Working Group, P802.15-03/02490r1-SG3a, Feb. 2003.

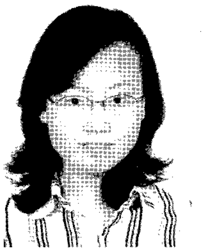

Yue Wang received her B.Sc. and M.Sc. degrees in Electrical and Computer Engineering from Xi'an Jiaotong University, China in 1999 and 2002, respectively, and her Ph.D. degree in Electrical and Computer Engineering from University of Victoria, Victoria, BC, Canada in 2006. She did her internship in the Wireless Communication and Networking department at Philips Research North America, Briarcliff Manor, NY during her Ph.D., and joined the advanced wireless research group at Toshiba Research Europe Ltd., Bristol, UK upon graduation. Her current research focuses on algorithms design for very high data rate wireless networks.

Xiaodai Dong received her B.Sc. degree in Information and Control Engineering from Xi'an Jiaotong University, China in 1992, her M.Sc. degree in Electrical Engineering from National University of Singapore in 1995 and her Ph.D. degree in Electrical and Computer Engineering from Queen's University, Kingston, ON, Canada in 2000. She is presently an associate professor and Canada research chair (Tier II) in Ultra-wideband Communications at the Department of Electrical and Computer Engineering, University of Victoria, Victoria, BC, Canada. Between 2002 and 2004, she was an assistant professor at the Department of Electrical and Computer Engineering, University of Alberta, Edmonton, AB, Canada. From 1999 to 2002, she was with Nortel Networks, Ottawa, ON, Canada and involved in the base transceiver design of the third-generation (3G) mobile communication systems. She is an associate editor for IEEE Transactions on Communications and an editor for Journal of Communications and Networks. Her research interests include communication theory, modulation and coding, and ultra-wideband radio.